

SUPPLEMENTARY INFORMATION

Bifunctional heterogeneous catalysts from biomass and waste polysaccharides for the conversion of CO₂ into cyclic carbonates

Adriano Parodi,^{*,§,a} Martina Vagnoni,^{*,§,a} Lucia Frontali,^a Cristiano Albonetti,^b Francesca De Giorgio,^b Alessio Mezzi,^c Elisabetta Petri,^a Chiara Samorì,^a Francesca Soavi,^a Giampiero Ruani,^b Paola Galletti^a

^aChemistry Department “Giacomo Ciamician”, University of Bologna. Via Selmi, 2, 40126, Bologna (Italy)

^bConsiglio Nazionale delle Ricerche, Istituto per lo Studio dei Materiali Nanostrutturati (CNR-ISMN). Via Piero Gobetti, 101 – 40129 Bologna (Italy)

^cConsiglio Nazionale delle Ricerche, Istituto per lo Studio dei Materiali Nanostrutturati (CNR-ISMN). Via Salaria km 29.300 - 00015 Monterotondo Scalo (Italy)

Contents

S1 Comparison of various carbon-based and biobased heterogeneous catalysts, for the synthesis of styrene carbonate from CO₂ and styrene oxide

S2 Char functionalization yields for each step (Table S2)

S3 Elemental analysis of the functionalized chars over different reaction conditions (Table S3a) and their application in the synthesis of SC (Table S3b)

S4 Elemental analysis of the chars functionalized with Bul and Octl over different conditions (Table S4a) and their application in the synthesis of SC (Table S4b)

S5 Elemental analysis of the cellulose functionalized avoiding pyrolysis and oxidation steps (Table S5a) and their application in the synthesis of SC (Table S5b)

S6 Weight of HC-FSD, HC-PC and HC-CA after each reaction cycle

S7 Recycling catalytic test for HC-FSD with 5 wt% of catalyst loading

S8 Elemental composition of the final catalysts HC-FSD after 5 cycles

S9 Raman characterization

S10 ATR-FTIR characterization of the starting materials

S11 Morphological characterization (SEM)

S12 Band assignment of the ATR-FTIR spectra of pristine cellulose- and sawdust-derived chars shown in Fig. 2a-d

S13 ¹H and ¹³C NMR spectra of isolated PRODUCT 2a (Table 6, entry 1)

S14 ^1H and ^{13}C NMR spectra of isolated PRODUCT 2b (Table 6, entry 2)

S15 ^1H and ^{13}C NMR spectra of isolated PRODUCT 2c (Table 6, entry 3)

S16 ^1H and ^{13}C NMR spectra of isolated PRODUCT 2d (Table 6, entry 4)

S17 ^1H and ^{13}C NMR spectra of isolated PRODUCT 2e (Table 6, entry 5)

S18 XPS quantitative analysis and BE value of the HCs

S19 HCs Active sites quantification

S20 Comparison of the spectra of C1s, O1s, N1s, Si2p and I3d of the HC-FSD and HC-FSD-5Cy samples

Bibliography

S1 Comparison of various carbon-based and biobased heterogeneous catalysts, for the synthesis of styrene carbonate from CO₂ and styrene oxide

Starting	Catalyst	w/w %	Co-catalyst	mol%	Pressure [MPa]	T [°C]	Time [h]	Yield ^a [%]	TON ^d	TOF [h ⁻¹]	Productivity [h ⁻¹]	Reference
Hard- and softwood residues		2.5	TBAB	1	1	110	6	71.9 (Conv.)	71,9	12,0	6,1	[1]
Graphene oxide		2.5	TBAI	1	0.1	100	27	94	94	3,5	1,5	[2]
					1	70	12	98	98	8,2	3,6	
Graphene oxide		2.9	-	-	2	120	3	56.9 (Sel. 96.2)	87,5	29,2	8,9	[3]
Cellulose		0.4 mol%	-	-	1.2	120	4	93	232,5	58,1	n.a.	[4]
Cellulose		0.8	-	-	1.5	130	5	96.1 (Sel. 96.9)	na	na	3,1	[5]
Lignin	Lignin	0.7 mol%	KI	2	2	140	12	87 ^c	43,5	3,6	3,6	[6]
Lignin		0.8	TBAB	10	1	110	3	90 ^c	9	3,0	1,5	[7]
Luffa sponge (lignocellulosic material)		8.3	TBAB	9	1	90	5	94 ^c (Sel. >99)	10,4	2,1	1,1	[8]
Chitosan		4.5	-	-	1.17	120	6	80 (Sel. >99)	57,2	9,5	4,1	[9]
Chitosan		6.9	TBAB	1	0.1	80	4	95 ^c	95,0	23,8	12,1	[10]
Mesoporous zeolite-chitosan		2.4	TBAI	2	1	100	6	77 ^b	63,1	10,5	4,7	[11]
Potato Starch		10	-	-	0.3	70	7	82 ^c	26.9	3.8	1.6	This work
Starch-Based Plastic Bags								88 ^c	26	3.7	1.7	
Pristine Cellulose								86 ^c	25.1	3.6	1.7	
Fir Sawdust								91 ^c	27.5	3.9	1.8	
Cellulose Acetate								86 ^c	26.9	3.8	1.7	
Post-Use Cigarette Filters								84 ^c	25.4	3.6	1.6	
Potato Starch		5	-	-	0.3	70	7	72 ^c	47.2	6.7	2.8	This work
Starch-Based Plastic Bags								79 ^c	46.9	6.7	3.1	
Pristine Cellulose								77 ^c	45.1	6.4	3.0	
Fir Sawdust								80 ^c	48.4	6.9	3.2	
Cellulose Acetate								77 ^c	48	6.9	3.0	
Post-Use Cigarette Filters								76 ^c	46.3	6.6	3.0	

^a Determined by GC.

^b Determined by ¹H NMR.

^c Isolated Yield.

^d Calculated on the Lewis Base species.

S2 Char functionalization yields for every step**Table S2** Four-step functionalization yield for every material tested

Reaction Step	Starting Material					
	FSD	PC	SBPB	PS	PUCF	CA
1 – Pyrolysis (%)	20	15.5	13	14	15	14.5
2 – Oxidation (%)	65	61	70	62	64	61
3 – Amination (%)^a	130	125	135	124	131	126
4 – Quaternarization (%)^a	113	108	112	109	115	110

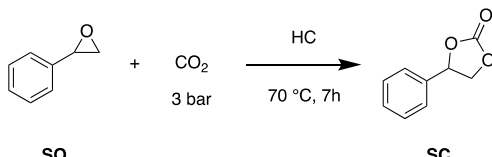
^a Yields of step 3 and 4 are higher than 100% due to addition of functional groups (APTES for step 3 and MeI for step 4) that increase char weight.

S3 Elemental analysis of the functionalized chars over different reaction conditions and their application in the synthesis of SC

Table S3a Elemental analysis of the functionalized chars from fir sawdust (FSD) over different reaction conditions (*mean wt% ± standard deviation of three independent replicates*)

Catalyst	Conditions	N (%)	C (%)	H (%)
A	1) 420 °C, 15h; 2) HNO ₃ , 85°C, 48h; 3) WET, APTES, EtOH, 80°C reflux, 24h; 4) MeI, EtOH 40°C, 16h	5.9 ± 0.1	34.7 ± 0.3	4.4 ± 0.2
B	1) 420 °C, 15h; 2) H ₂ SO ₄ , KMnO ₄ , 85 °C, 24h; 3) WET, APTES, EtOH, 80°C reflux, 24h; 4) MeI, EtOH 40°C, 16h	0.4 ± 0.1	63.5 ± 0.4	2.6 ± 0.1
C	1) 420 °C, 15h; 2) HNO ₃ /H ₂ SO ₄ (1:3), 85°C, 6h; 3) WET, APTES, EtOH, 80°C reflux, 24h; 4) MeI, EtOH 40°C, 16h	4.3 ± 0.2	51.8 ± 0.5	3.8 ± 0.2
D	1) 550 °C, 15h; 2) H ₂ O ₂ , 85 °C, 24h; 3) APTES, EtOH:H ₂ O (96/4), 80°C 4) MeI, EtOH 40°C, 16h	0.6 ± 0.2	81.8 ± 0.6	1.4 ± 0.1
E	1) 420 °C, 15h; 2) H ₂ O ₂ , 85 °C, 24h; 3) APTES, EtOH (no H₂O), 80°C; 4) MeI, EtOH 40°C, 16h	3.1 ± 0.1	36.0 ± 0.4	4.7 ± 0.1
F	1) 420 °C, 15h; 2) H ₂ O ₂ , 85 °C, 24h; 3) APTES, EtOH:H₂O (90/10) , 80°C; 4) MeI, EtOH 40°C, 16h	5.6 ± 0.1	31.9 ± 0.6	4.3 ± 0.2
G	1) 420 °C, 15h; 2) APTES, EtOH:H ₂ O (96/4), 80°C	0.08 ± 0.05	75.7 ± 0.2	2.5 ± 0.2
H	1) 420 °C, 15h; 2) APTES, EtOH:H ₂ O (96/4), 80°C 3) MeI, EtOH 40°C, 16h	0.05 ± 0.03	74.9 ± 0.2	2.7 ± 0.1

Table S3b Results for carbonation reaction using catalyst obtained from fir sawdust (FSD) produced over different conditions (Table S.3a)



Entry	Catalyst	SC [%] ^{b,c}
1 ^a	A	86
2	B	0
3	C	71
4	D	0
5	E	21
6	F	14
7	H	0

^a Reaction conditions: 0.875 mmol SO (100 µL), HC (10% w/w), autoclave.

^b Isolated Yields are given, after purification of the reaction crude by flash column chromatography. Yield of SC was the average after two runs.

^c Selectivity was >99% for all entries. It was determined by ¹H NMR spectroscopy using mesitylene as internal standard.

- Oxidation step is of fundamental importance to efficiently anchor -NH₂ functionalities and produce an active catalyst (Table S3a, entry G).

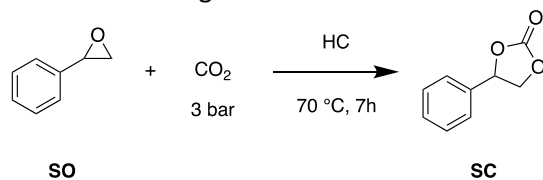
- Hydrolytic condensation of APTES was also conducted, using third step optimized conditions (APTES, EtOH:H₂O (96/4), 80°C) without the presence of the char: no polymeric solid from APTES self-condensation was obtained, resulting in a clear transparent solution.

S4 Elemental analysis of the char functionalized with Bul and Octl over different conditions (Table S4a) and their application in the synthesis of SC (Table S4b)

Table S4a Elemental analysis of the optimization of reaction conditions for Bul and Octl anchoring

Label	Conditions	N (wt%)	C (wt%)	H (wt%)
G	Bul, EtOH 40°C, 16H	6.3 ± 0.2	39.6 ± 0.3	5.2 ± 0.2
H	Octl, EtOH 40°C, 16H	6.3 ± 0.1	40.3 ± 0.2	5.3 ± 0.2
I	Bul, 80°C, 16H	5.2 ± 0.1	33.0 ± 0.4	4.5 ± 0.1
J	Octl, 80°C, 16H	5.4 ± 0.2	36.3 ± 0.3	4.9 ± 0.2
K	Bul, 120°C, 16H	4.7 ± 0.1	34.2 ± 0.2	4.7 ± 0.1
L	Octl, 120°C, 16H	4.9 ± 0.1	41.2 ± 0.5	5.4 ± 0.2

Table S4b Results for carbonation reaction using Bul and Octl functionalized catalysts



Entry ^a	Catalyst	SC [%] ^{b,c}
1	G	26
2	H	15
3	I	65
4	J	61
5	K	79
6	L	84

^a Reaction conditions: 0.875 mmol SO (100 µL), HC (10% w/w), autoclave.

^b Isolated Yields are given, after purification of the reaction crude by flash column chromatography. Yield of SC was the average after two runs.

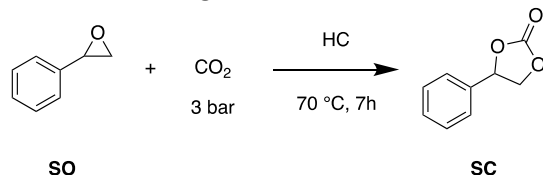
^c Selectivity was >99% for all entries. It was determined by ¹H NMR spectroscopy using mesitylene as internal standard.

S5 Elemental analysis of the cellulose functionalized avoiding pyrolysis and oxidation steps (Table S5a) and their application in the synthesis of SC (Table S5b)

Table S5a Elemental analysis of the optimization of reaction conditions for cellulose functionalization avoiding step 1 and 2 (*mean wt% ± standard deviation of three independent replicates*)

Label	Conditions	N (%)	C (%)	H (%)
M	1) APTES (4.4%), EtOH:H ₂ O (96/4), 80°C; 4h; 2) Mel, EtOH 40°C, 16h	0.2 ± 0.05	38 ± 0.2	5.8 ± 0.1
N	1) APTES (35%), EtOH:H ₂ O (96/4), 120°C; 24h; 2) Mel, EtOH 40°C, 16h	2.1 ± 0.1	32.3 ± 0.3	5.4 ± 0.1
O	1) APTES:H ₂ O (1/1), 140°C; 24h; 2) Mel, EtOH 40°C, 16h	3.75 ± 0.1	24.4 ± 0.2	5.3 ± 0.1

Table S5b Results for carbonation reaction using cellulose functionalized catalysts avoiding step 1 and 2



Entry ^a	Catalyst	SC [%] ^{b,c}
1	M	0
2	N	40
3	O	79

^a Reaction conditions: 0.875 mmol SO (100 µL), HC (10% w/w), autoclave.

^b Isolated Yields are given, after purification of the reaction crude by flash column chromatography. Yield of SC was the average after two runs.

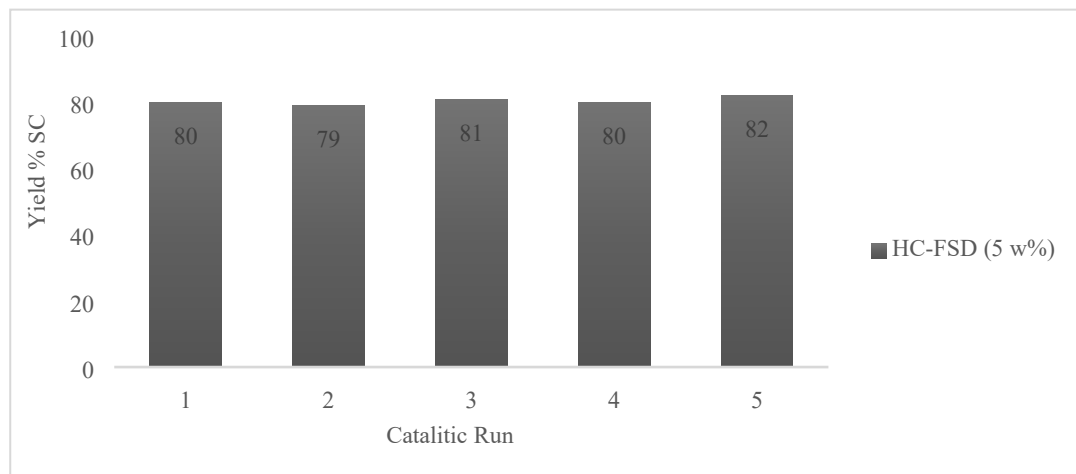
^c Selectivity was >99% for all entries. It was determined by ¹H NMR spectroscopy using mesitylene as internal standard.

S6 Weight of HC-FSD, HC-PC and HC-CA after each reaction cycle

Table S6 Weight of HC-FSD, HC-PC and HC-CA after each reaction cycle

	HC-FSD		HC-PC		HC-CA	
	Weight [mg]	Variation [%]	Weight [mg]	Variation [%]	Weight [mg]	Variation [%]
I cycle	10.5	-	10.5	-	10.5	-
II cycle	14.1	141	12.2	122	14.4	144
III cycle	13.7	137	13.1	131	14	140
IV cycle	13.3	133	12.9	129	14.2	142
V cycle	13.2	132	13.3	133	12.8	128

S7 Recycling catalytic test for HC-FSD with 5 wt% of catalyst loading



S8 Elemental composition of the final catalysts HC-FSD after 5 cycles

Table S8 Elemental composition of the final catalysts HC-FSD after 5 cycles (mean wt% \pm standard deviation of three independent replicates)

Starting Material	catalyst	N (%)	C (%)	H (%)
Fir Sawdust	HC-FSD-5Cy	4.0 \pm 0.1	48.3 \pm 0.4	4.9 \pm 0.1

S9 Raman characterization

Fig. S5 shows the comparison of the Raman spectra of the six catalysts obtained from the different starting materials. While the spectra of cellulose HC-C and cellulose acetate HC-CA display no peaks (spectra are dominated by a strong structure less luminescent background), those of the catalysts potato starch HC-PS, starch-based plastic bag HC-SBPB and post-use cigarette filters HC-PUCF show G and D bands at around 1600 cm^{-1} and 1370 cm^{-1} , respectively, related to the in-plane C-C vibrations of sp^2 -bonded carbon atoms in graphitic-like structures and to the out-of-plane C-C vibrations due to structural defects in the graphitic structure.^{12,13,14}

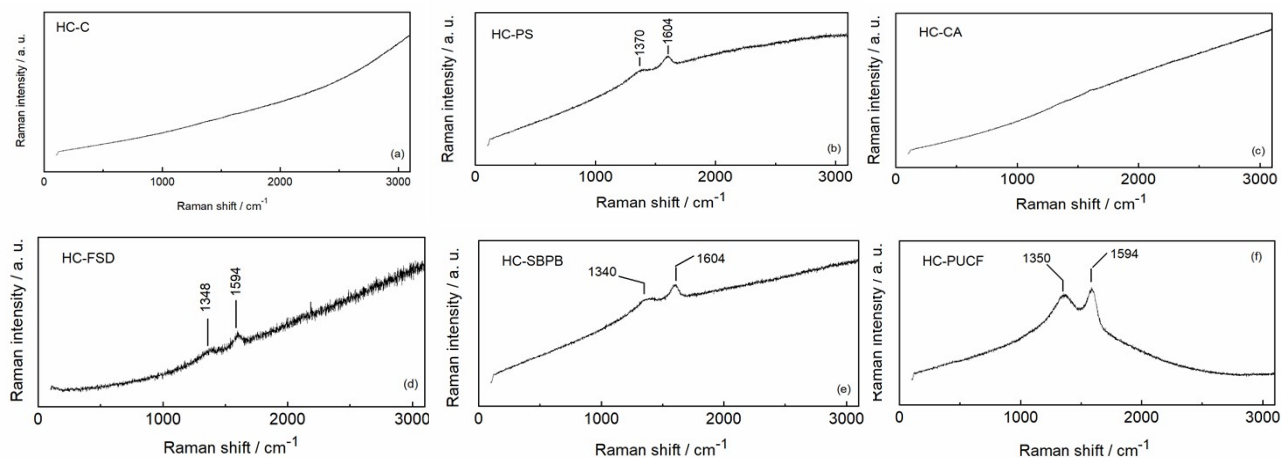


Fig. S9 Comparison of the Raman spectra of the six catalysts obtained from different starting materials ($\lambda_{\text{exc}} = 488\text{ nm}$): (a) pristine cellulose HC-PC; (b) potato starch HC-PS; (c) cellulose acetate HC-CA; (d) fir sawdust HC-FSD; (e) starch-based plastic bag HC-SPB; (f) post-use cigarette filters HC-PUCF.

S10 ATR-FTIR characterization of the starting materials

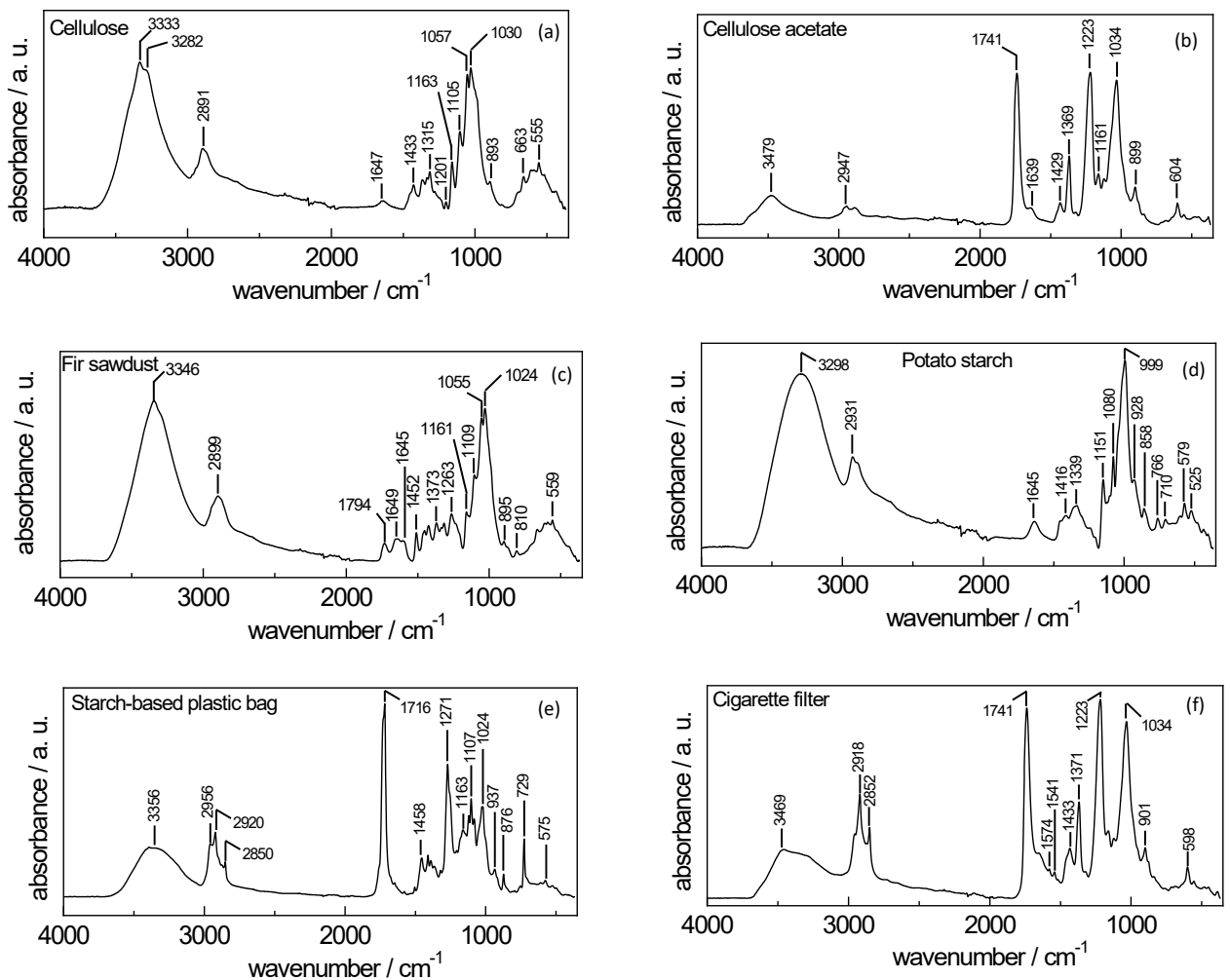


Fig. S10 ATR-FTIR spectra of catalyst precursors: (a) pristine cellulose; (b) cellulose acetate; (c) fir sawdust; (d) potato starch; (e) starch-based plastic bag; (f) post-use cigarette filter.

S11 Morphological characterization

The six catalysts, i.e. HC-based samples obtained from different starting materials, were imaged by Scanning Electron Microscopy (SEM) for understanding if the catalyst morphology could affect the yield of CO₂ conversion in the cyclic carbonate reaction. Catalysts images collected at low magnification (x 80) (Fig. S11) suggest three archetypical morphologies: small-medium aggregates with crystal-like shape (a, b, c), big aggregates with crystal-like shape (d, e, f) and big aggregates with no regular shape (g). By comparing SEM images to yield results, no straightforward correlation is observed amongst them.

This finding is also confirmed by comparing images collected at higher magnifications (x 700 and x 2.5k) (Fig. S11'). By inspecting morphologies at x 700, crystal-like aggregates are smaller in HC-CA (S11'a) rather than HC-SBPB (S11'b), with no significant morphological differences even at the highest magnification (i.e. x 2.5k, S11'c and S11'd).

Figure S11'' compares SEM images collected at x 2.5k for post-use cigarette filters HC-PUCF (S11''a) and fir sawdust HC-FSD (S11''b). The catalyst HC-PS has a more compact surface respect to HC-PUCF one. Such a compact surface of HC-FSD is partly maintained also in recycled HC-FSD after five recycling runs (S11''c).

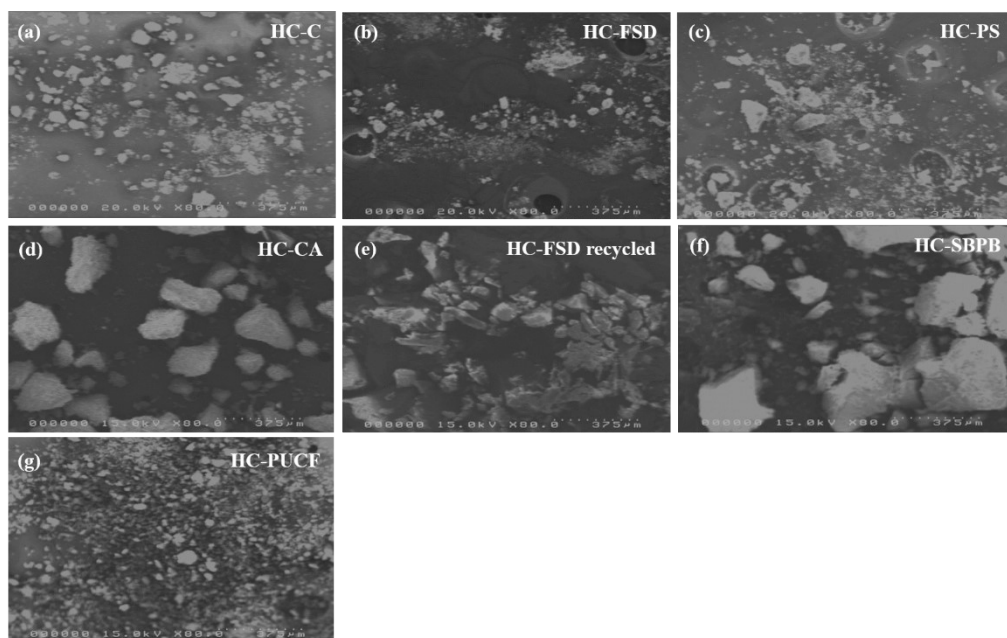


Fig. S11 SEM images (x 80) of the catalysts: (a) cellulose HC-C; (b) fir sawdust HC-FSD; (c) potato starch HC-PS; (d) cellulose acetate HC-CA; (e) fir sawdust HC-FSD recycled after five recycling runs; (f) starch-based plastic bag HC-SPB; (g) post-use cigarette filters HC-PUCF.

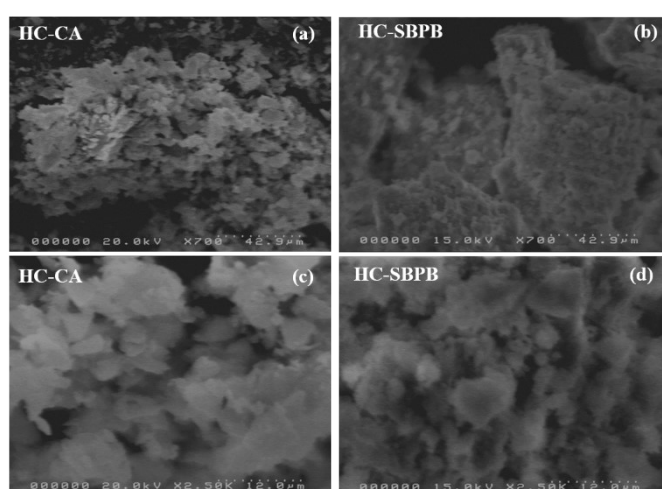


Fig. S11' SEM images of the catalysts (a, c) cellulose acetate HC-CA and (b, d) starch-based plastic bag HC-SBPB at different magnifications: (a, b) x 700 and (c, d) x 2.5k.

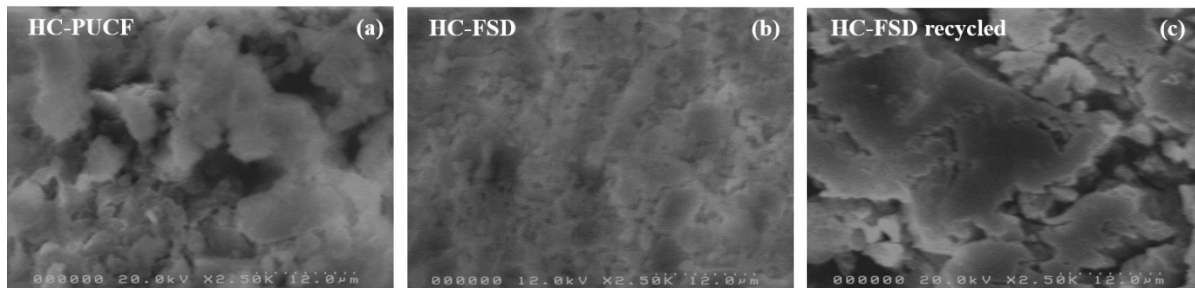
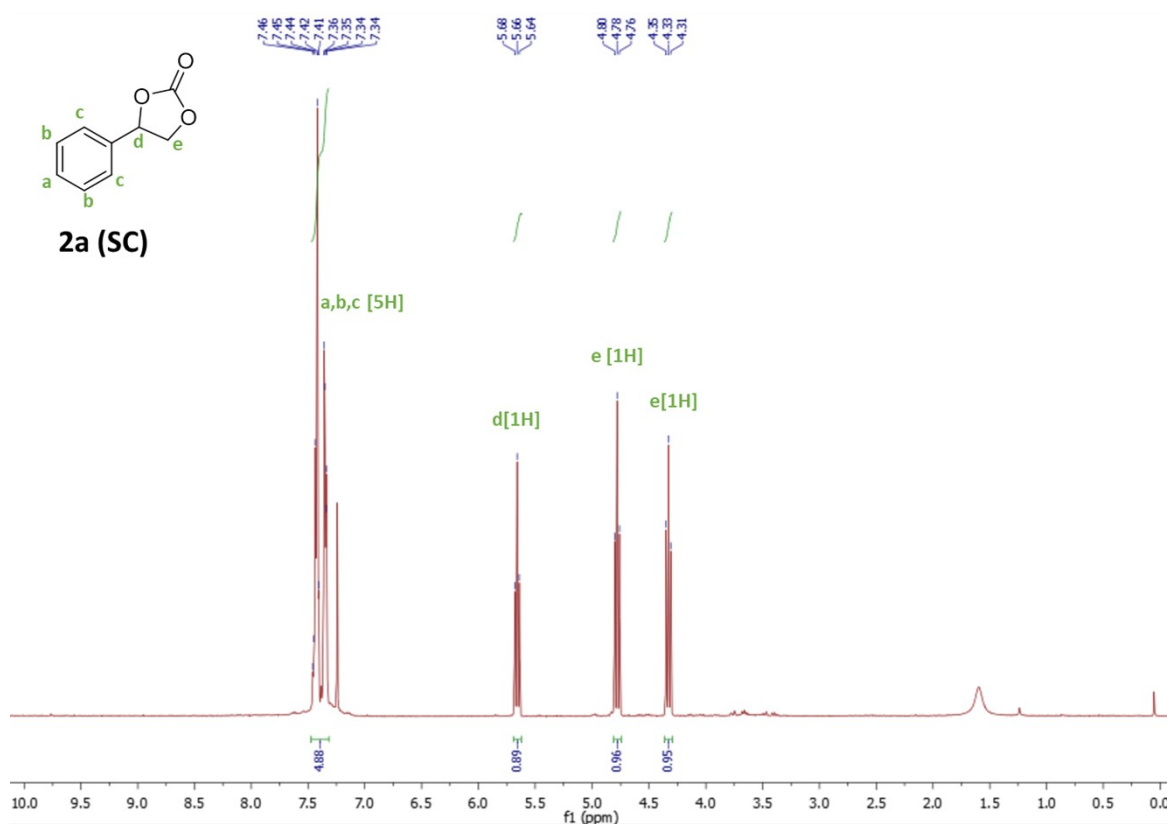


Fig. S11'' SEM images at x 2.5k of the catalysts (a) post-use cigarette filters HC-PUCF, (b) fir sawdust HC-FSD and (c) fir sawdust HC-FSD recycled after five recycling runs.

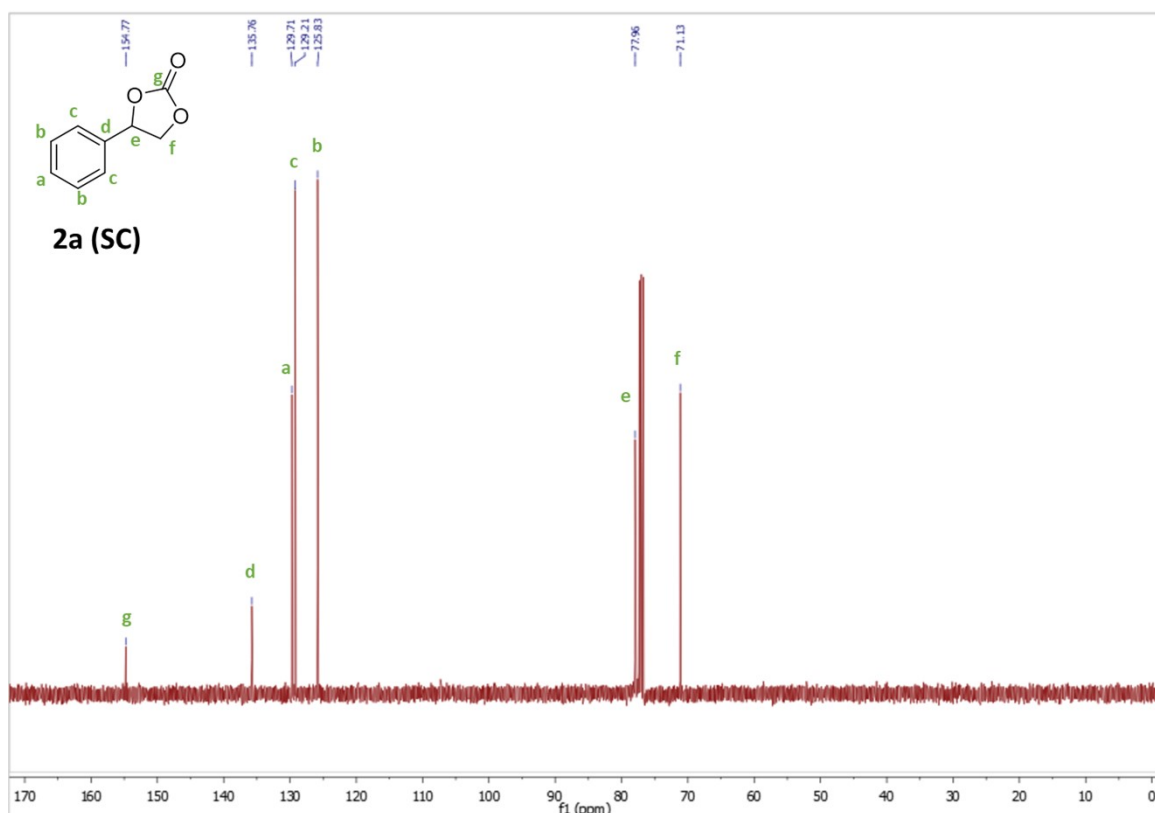
S12 Band assignment of the ATR-FTIR spectra of pristine cellulose- and sawdust-derived samples shown in Fig. 2a-d.^{15–21}

Band position (cm ⁻¹)	Assignment
1698	Stretching of conjugate C=O within the ring of polycyclic aromatic systems
1584	Skeletal vibrations involving C-C stretching within the ring of polycyclic aromatic systems
1169	C-O stretch of phenols
875 - 750	Out-of-plane ("oop") bending of C-H bond of polycyclic aromatic hydrocarbon systems
1710	C=O stretching of carboxy groups
1375	In-plane O-H bending of phenol OH groups
1215	C-O stretching of phenol OH groups
3500 - 2500	O-H stretching of the phenol OH and Si-OH groups; N-H stretching vibrations
1110/1040	C-N stretching of primary amines; Si-O-C (aliphatic), Si-O stretching vibrations
920	Si-OH stretch
460	Si-O rocking vibrations
3390	N-H stretching vibrations of ammonium salt

S13 ^1H and ^{13}C NMR spectra of isolated **PRODUCT 2a** (Table 6, entry 1).

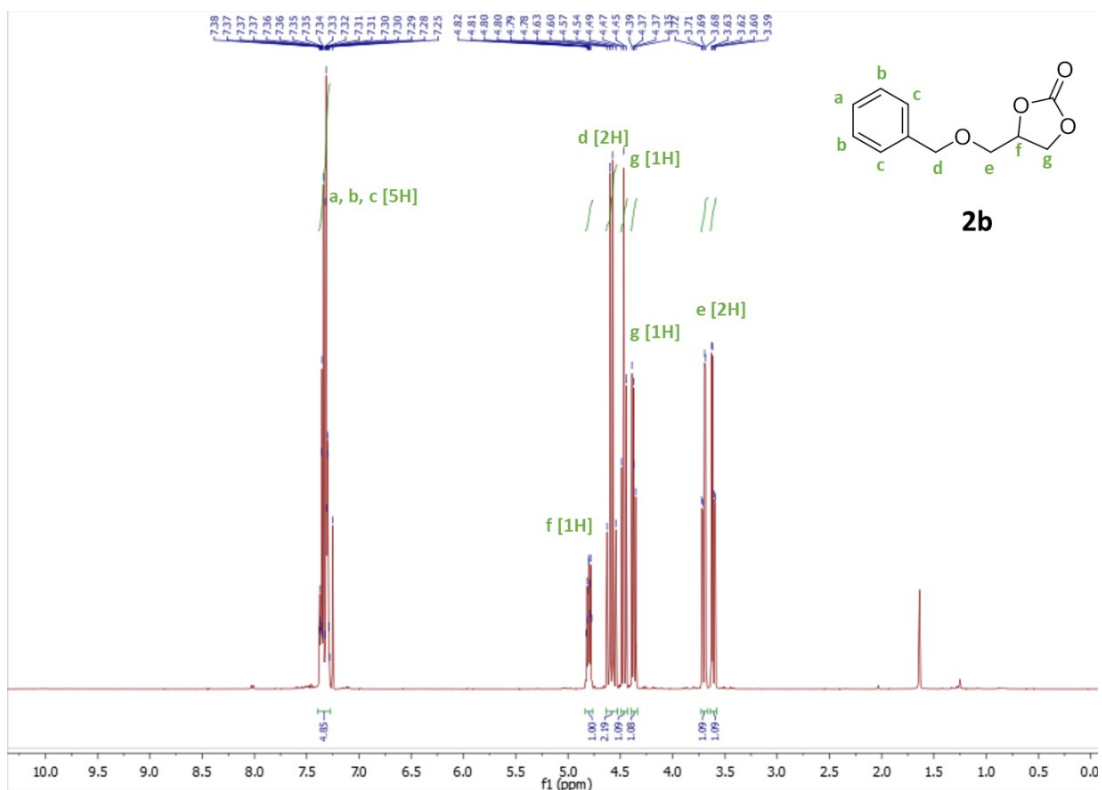


2a. ^1H NMR (400 MHz, CDCl_3) δ 7.46 - 7.34 (m, 5H), 5.66 (t, $J = 8.0$ Hz, 1H), 4.78 (t, $J = 8.4$ Hz, 1H), 4.33 (dd, $J = 8.5, 8.0$ Hz, 1H).

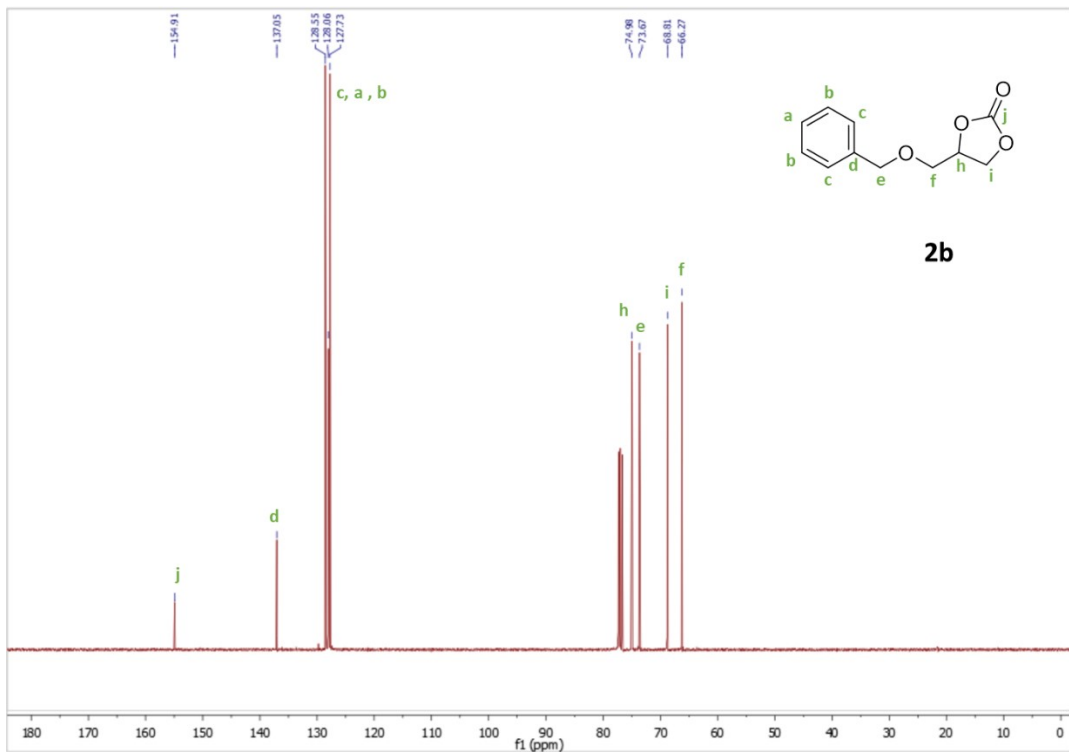


2a. ^{13}C NMR (100 MHz, CDCl_3) δ 154.77, 135.76, 129.71, 129.21, 125.83, 77.96, 71.13

S14 ^1H and ^{13}C NMR spectra of isolated **PRODUCT 2b** (Table 6, entry 2).

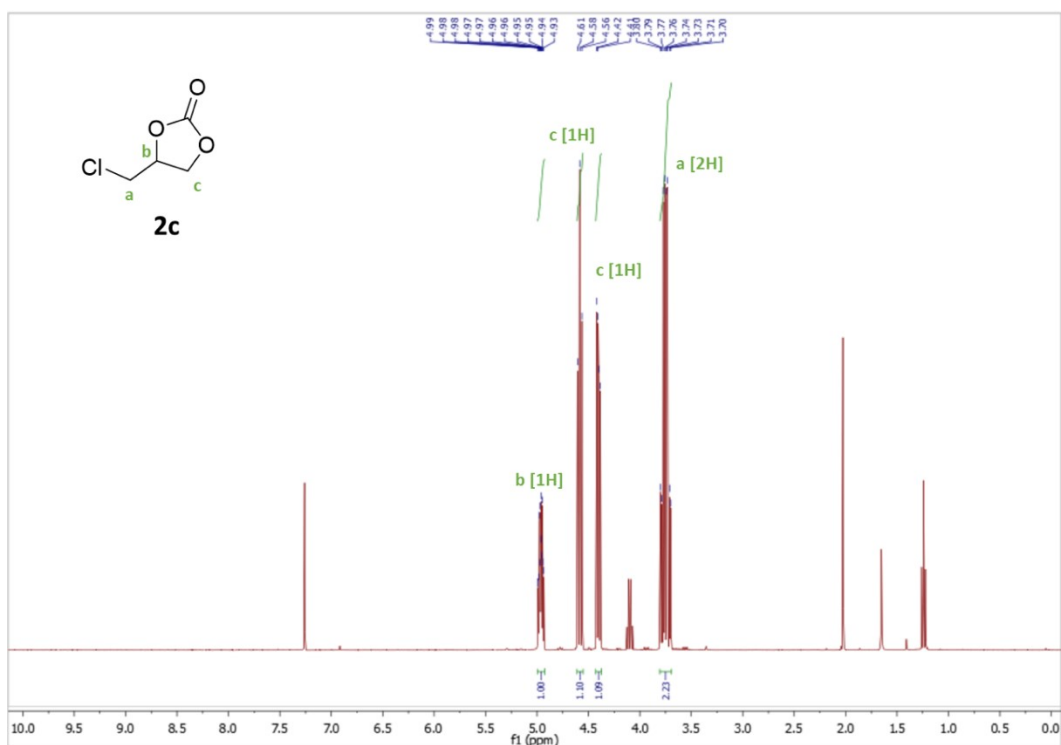


2b. ^1H NMR (400 MHz, CDCl_3) δ 7.38 – 7.25 (m, 5H), 4.879 (ddt, J = 7.9, 6.1, 3.9 Hz, 1H), 4.60 (m, 2H), 4.49 (t, J = 8.4 Hz, 1H), 4.37 (dd, J = 8.4, 6.1 Hz, 1H), 3.70 (dd, J = 10.9, 4.0 Hz, 1H), 3.61 (dd, J = 10.9, 3.8 Hz, 1H).
Impurities signals: H_2O (1.56, s).

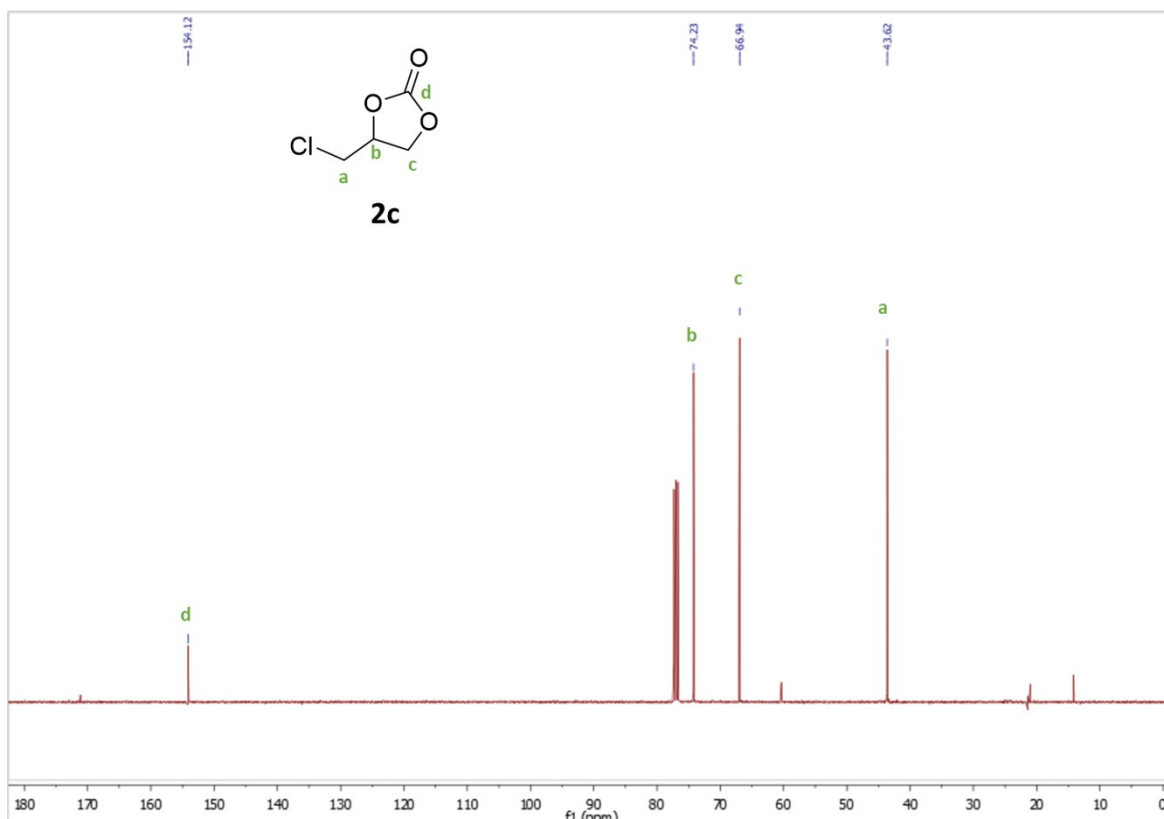


2b. ^{13}C NMR (100 MHz, CDCl_3) δ 154.91, 137.05, 128.55, 128.06, 127.73, 74.98, 73.67, 68.81, 66.27.

S15 ^1H and ^{13}C NMR spectra of isolated **PRODUCT 2c** (Table 6, entry 3).

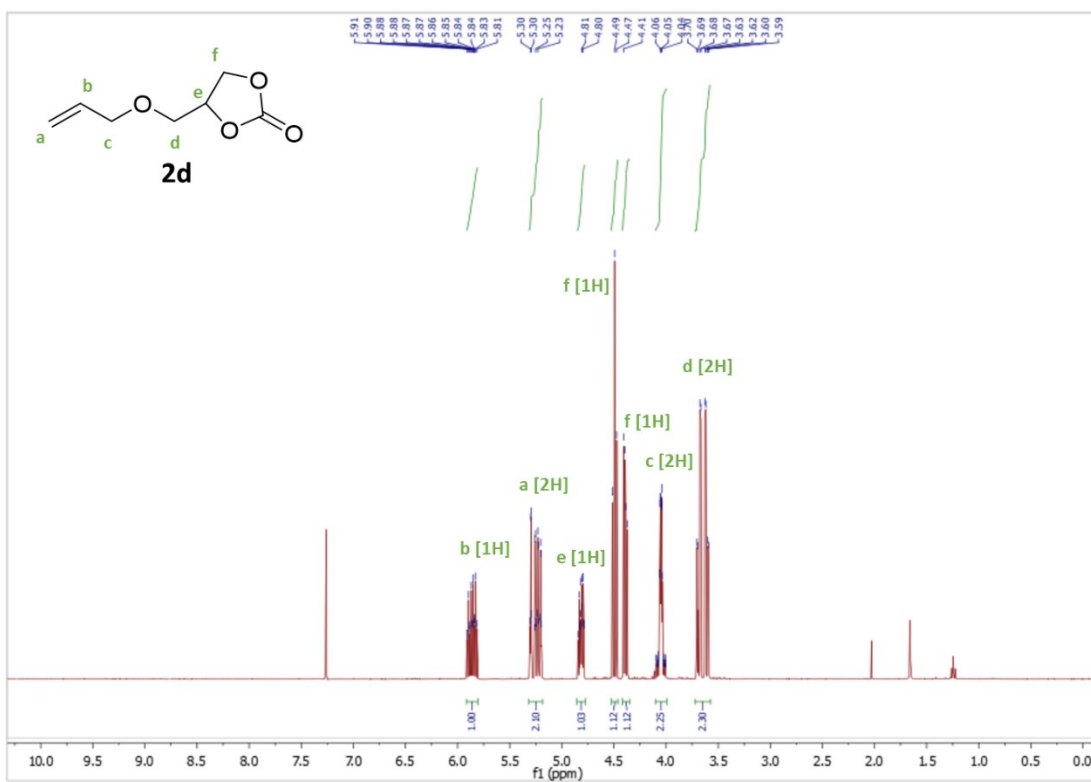


2c. ^1H NMR (400 MHz, CDCl_3) δ 4.96 (m, 1H), 4.58 (t, $J = 8.6$ Hz, 1H), 4.4 (dd, $J = 8.9, 5.7$ Hz, 1H), 3.75 (m, 2H).
Impurities signals: H_2O (1.56, s); AcOEt (2.05, s; 4.12, q; 1.26, t)

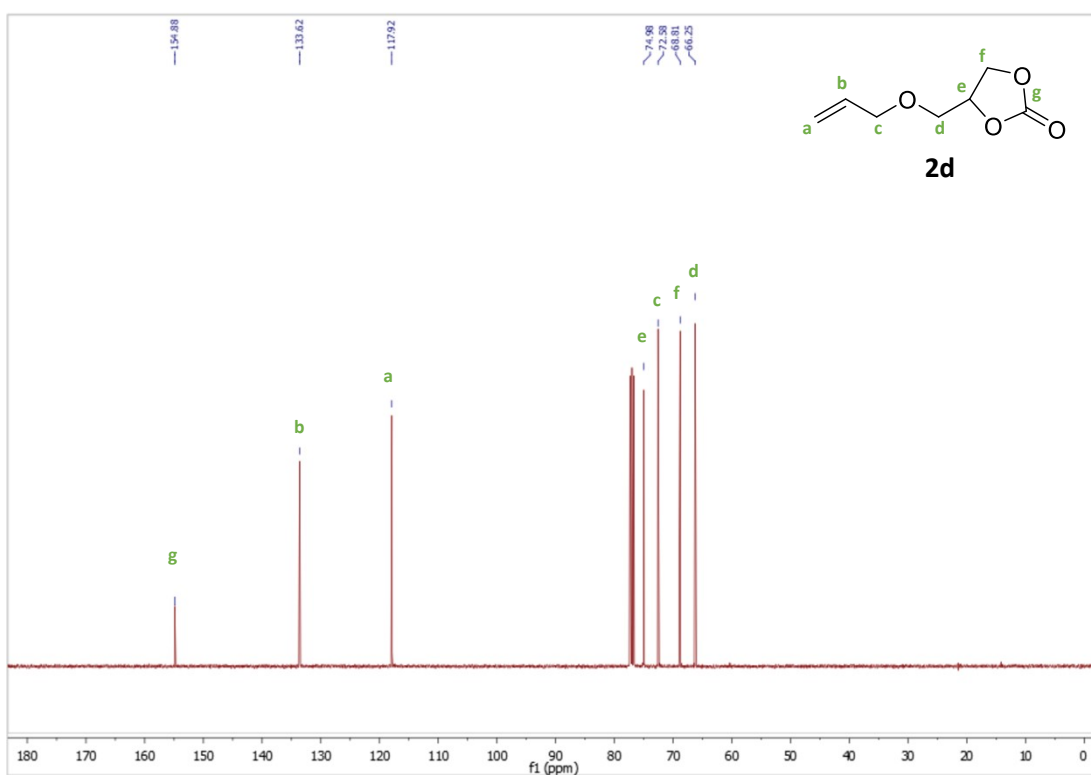


2c. ^{13}C NMR (100 MHz, CDCl_3) δ 154.12, 74.23, 66.94, 43.62.
Impurities signals: AcOEt (21.04, 171.36, 60.49, 14.19)

S16 ^1H and ^{13}C NMR spectra of isolated **PRODUCT 2d** (Table 6, entry 4).

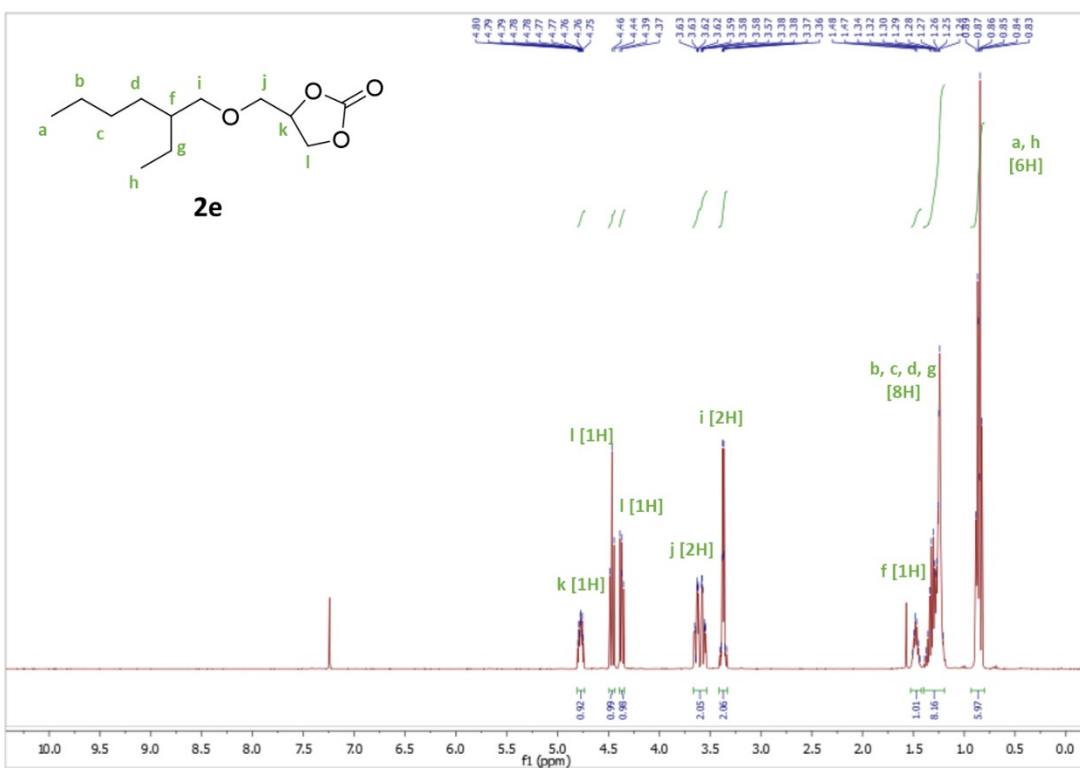


2d. ^1H NMR (400 MHz, CDCl_3) δ 5.86 (ddd, $J = 22.8, 10.8, 5.6$ Hz, 1H), 5.30 - 5.23 (m, 2H), 4.8 (ddt, $J = 8.1, 6.1, 3.9$ Hz, 1H), 4.48 (t, $J = 8.4$ Hz, 1H), 4.41 (dd, $J = 8.3, 6.1$ Hz, 1H), 4.05 (m, 2H), 3.70-3.59 (m, 2H).
Impurities signals: H_2O (1.56, s); AcOEt (2.05, s; 4.12, q; 1.26, t)



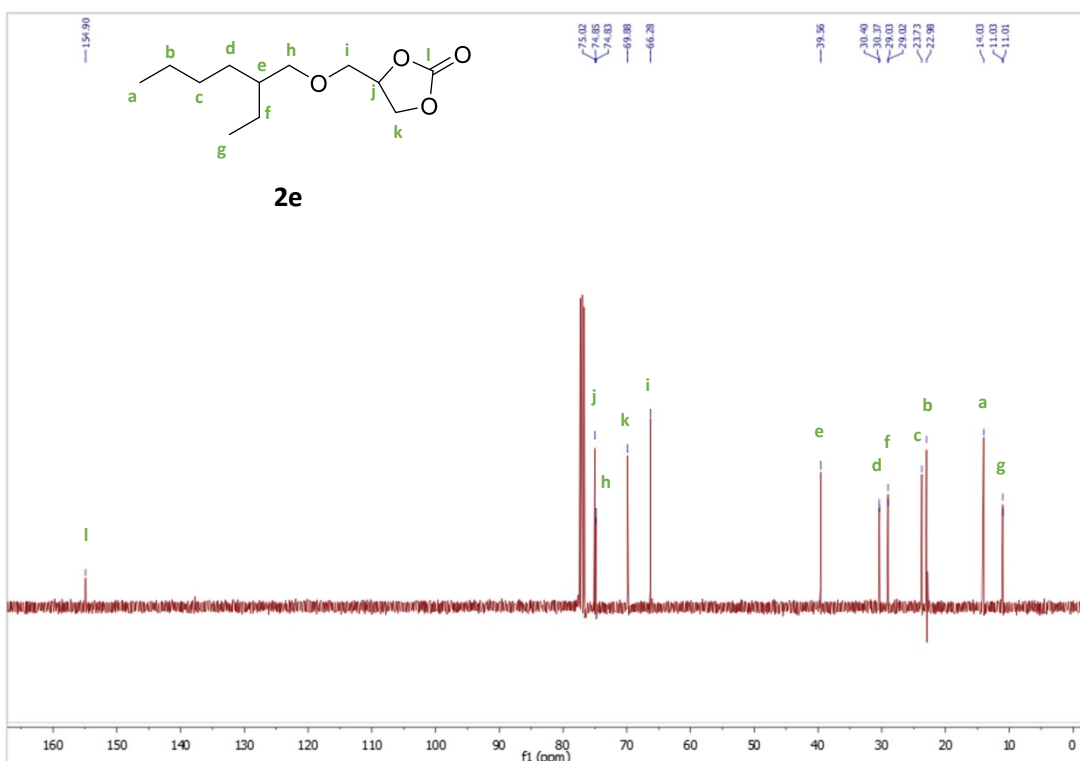
2d. ^{13}C NMR (100 MHz, CDCl_3) δ 154.88, 133.62, 117.92, 74.98, 72.58, 68.81, 66.25.

S17 ^1H and ^{13}C NMR spectra of isolated **PRODUCT 2e** (Table 6, entry 5).



2e. ^1H NMR (400 MHz, CDCl_3) δ 4.82 -4.76 (m, 1H), 4.46 (t, $J = 8.3$ Hz, 1H), 4.39 (dd, $J = 8.3, 6.0$ Hz, 1H), 3.62 (m, 2H), 3.39 (dd, $J = 5.7, 1.9$ Hz, 2H), 1.55 -1.53 (m, 1H), 1.38 -1.23 (m, 8H), 0.883- 0.89(m, 6H).

Impurities signals: H_2O (1.56, s).



2e. ^{13}C NMR (100 MHz, CDCl_3) δ 154.90, 75.02, 74.84, 69.88, 66.28, 39.56, 30.40, 29.03, 23.73, 22.98, 14.03, 11.02.

S18 XPS quantitative analysis and BE value of the HCs

Table S18a. XPS quantitative analysis and BE value of the sample HC-FSD.

Name	Peak BE	FWHM eV	Area (P) CPS.eV	Atomic %	Assignment
C1s - 1	285.0	1.68	14274.1	21.6	C - C
C1s - 2	286.8	1.68	11544.59	17.5	C - O, C - N
C1s - 3	287.9	1.68	5152.27	7.8	C = O
C1s - 4	288.7	1.68	2006.11	3.0	-COOH(R)
I3d5	618.5	1.61	78953.9	6.4	I ⁻
N1s - 1	399.8	2.64	710.58	0.6	Amine group
N1s - 2	402.4	2.64	7375.71	6.4	Ammonium group
O1s - 1	532.4	1.74	34327.09	18.8	C - O, C = O
O1s - 2	532.4	1.74	5686.7	3.1	Silicates
O1s - 3	534.5	1.74	1376.96	2.6	Si - O
Si2p3	103.0	1.95	664.86	10.8	APTES

Table S18b. XPS quantitative analysis and BE value of the sample HC-FSD (after recycling).

Name	Peak BE	FWHM eV	Area (P) CPS.eV	Atomic %	Assignment
C1s - 1	285.0	1.69	20053.63	54.3	C - C
C1s - 2	286.7	1.69	5536.75	15.0	C - O, C - N
C1s - 3	289.0	1.69	864.43	2.3	-COOH(R)
I3d5 - 1	618.2	1.99	1237.68	0.9	I ⁻
N1s - 1	399.9	2.02	1099.69	1.7	Amine group
N1s - 2	402.6	2.02	513.01	0.8	Ammonium group
O1s - 1	532.2	2.24	18529.00	18.2	C - O, C = O
O1s - 2	533.9	2.24	2154.29	2.1	silicates
Si2p3	102.6	1.75	1122.57	5.4	APTES

Table S18c. XPS quantitative analysis and BE value of the sample HC-PS.

Name	Peak BE	FWHM eV	Area (P) CPS.eV	Atomic %	Bond
C1s - 1	285.0	1.70	12850.03	21.8	C - C
C1s - 2	286.6	1.70	10377.10	17.6	C - O, C - N
C1s - 3	288.1	1.70	5205.01	8.8	C = O
C1s - 4	289.6	1.70	1740.05	3.0	-COOH(R)
C1s - 5	292.1	1.70	487.18	0.8	Shake-up satellite
I3d5 - 1	618.9	1.63	60850.41	5.7	I ⁻
I3d5 - 2	620.8	1.63	6615.38	0.6	I - O
N1s - 1	398.8	2.87	938.52	0.9	Amine group
N1s - 2	402.0	2.87	6826.07	6.6	Ammonium group
O1s - 1	532.5	1.85	30030.93	18.5	C - O, C = O
O1s - 2	534.2	1.85	4921.60	3.0	silicates
O1s - 3	531.0	1.85	3495.40	2.2	Si - O - Si
Si2p3 - 1	103.0	1.97	2576.84	7.8	APTES
Si2p3 - 2	105.2	1.96	895.26	2.7	silicates

Table S18d. XPS quantitative analysis and BE value of the sample HC-CA.

Name	Peak BE	FWHM eV	Area (P) CPS.eV	Atomic %	Bond
C1s – 1	285.0	1.76	6896.08	21.9	C – C
C1s – 2	286.5	1.76	6263.82	19.9	C – O, C – N
C1s – 3	288.2	1.76	2230.39	7.1	C = O
C1s – 4	290.1	1.76	544.44	1.7	-COOH(R)
I3d5 – 1	618.8	1.68	35722.30	6.2	I ⁻
I3d5 – 2	620.7	1.68	3031.15	0.5	I – O
N1s – 1	399.6	2.54	566.52	1.0	Amine group
N1s – 2	402.0	2.54	3609.76	6.5	Ammonium group
O1s – 1	532.4	1.92	17358.01	20.0	C – O, C = O
O1s – 2	530.6	1.92	1049.03	1.2	Si – O – Si
O1s – 3	534.1	1.92	2169.26	2.5	silicates
Si2p3 – 1	102.7	1.74	1551.33	8.8	APTES
Si2p3 – 2	104.3	1.74	437.60	2.5	silicates

Table S18e. XPS quantitative analysis and BE value of the sample HC-SBPB.

Name	Peak BE	FWHM eV	Area (P) CPS.eV	Atomic %	Bond
C1s – 1	285.0	1.69	11813.17	22.3	C – C
C1s – 2	286.6	1.69	10158.85	19.2	C – O, C – N
C1s – 3	288.2	1.69	4500.28	8.5	C = O
C1s – 4	289.8	1.69	1256.19	2.4	-COOH(R)
I3d5 – 1	618.8	1.67	63398.50	6.6	I ⁻
I3d5 – 2	620.7	1.67	6726.17	0.7	I – O
N1s – 1	399.6	2.84	286.58	0.3	Amine group
N1s – 2	402.0	2.84	6082.69	6.6	Ammonium group
O1s – 1	532.4	1.91	27429.85	18.8	C – O, C = O
O1s – 2	534.3	1.91	4643.95	3.2	silicates
O1s – 3	530.6	1.91	1568.21	1.1	Si – O – Si
Si2p3 – 1	102.8	1.75	1983.93	6.7	APTES
Si2p3 – 2	104.4	1.75	1085.04	3.7	silicates

Table S18f. XPS quantitative analysis and BE value of the sample HC-PUCF

Name	Peak BE	FWHM eV	Area (P) CPS.eV	Atomic %	Bond
C1s – 1	285.0	1.82	9037.37	25.3	C – C
C1s – 2	286.6	1.82	6357.14	17.8	C – O, C – N
C1s – 3	288.3	1.82	2308.84	6.5	C = O
C1s – 4	289.8	1.82	599.36	1.7	-COOH(R)
I3d5 – 1	618.8	1.72	41996.72	6.4	I ⁻
I3d5 – 2	620.8	1.72	4087.63	0.6	I – O
N1s – 1	399.6	2.68	635.57	1.0	Amine group
N1s – 2	401.9	2.68	4322.40	6.9	Ammonium group
O1s – 1	532.4	1.83	18374.52	18.6	C – O, C = O
O1s – 2	530.8	1.83	1786.16	1.8	Si – O – Si
O1s – 3	534.2	1.83	2645.43	2.7	silicates
Si2p3 – 1	102.7	1.85	1289.44	6.5	APTES
Si2p3 – 2	104.2	1.85	854.09	4.3	silicates

Table S18g. XPS quantitative analysis and BE value of the sample HC-PC.

Name	Peak BE	FWHM eV	Area (P) CPS.eV	Atomic %	Bond
C1s – 1	285.0	1.74	11370.10	24.9	C – C
C1s – 2	286.4	1.74	8443.04	18.5	C – O, C – N
C1s – 3	287.9	1.74	2273.89	5.0	C = O
C1s – 4	289.2	1.74	816.97	1.8	-COOH(R)
I3d5	618.8	1.64	56631.25	6.8	I ⁻
N1s – 1	399.3	2.28	870.71	1.1	Amine group
N1s – 2	401.9	2.28	5377.63	6.7	Ammonium group
O1s	532.4	2.10	30601.19	24.3	C – O, C = O
Si2p	103.3	2.18	4206.96	10.9	APTES

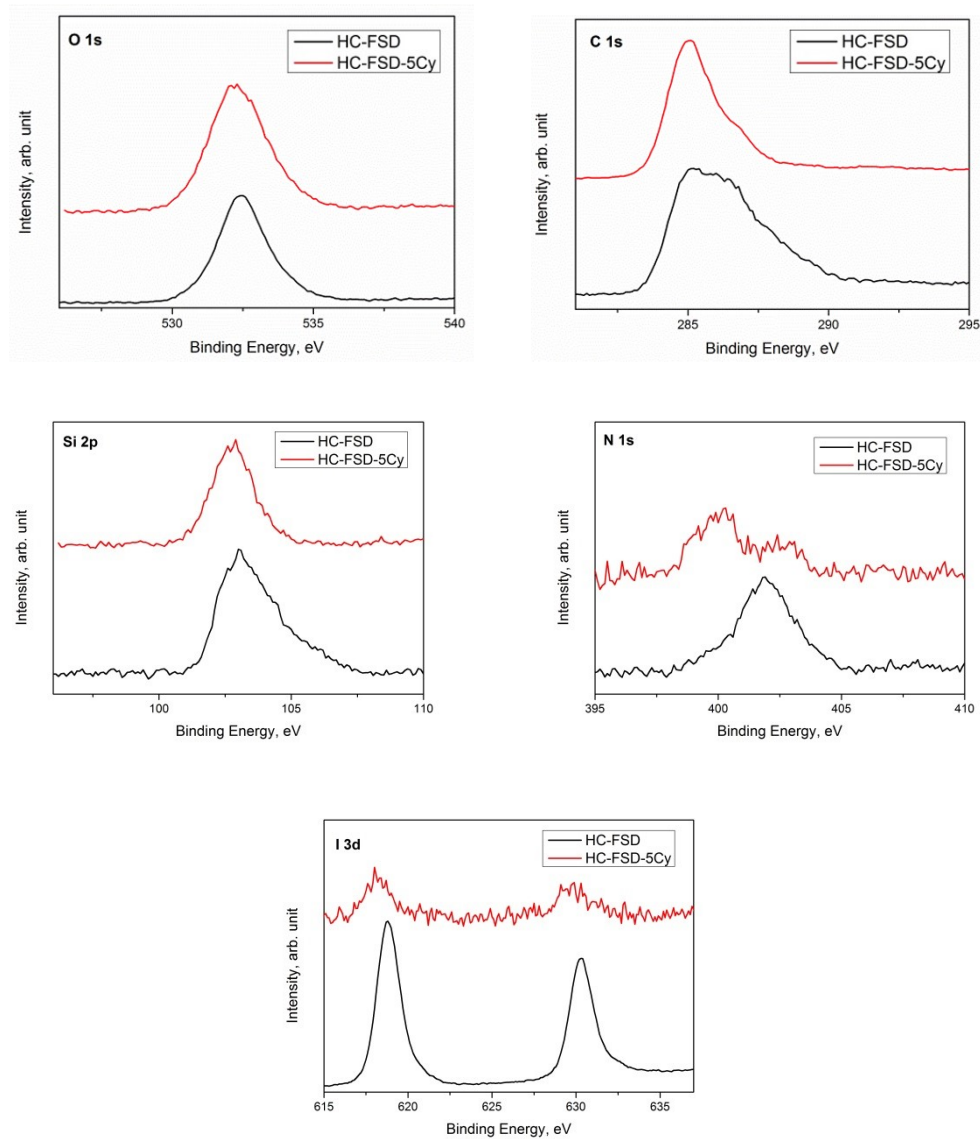
S19 HCs active sites quantification

Table S19. HCs I⁻ active sites (mmol/g)

Catalyst	I ⁻ Active site (mmol/g)
HC-FSD	2.9
HC-PS	2.7
HC-CA	2.8
HC-SBPB	3.0
HC-PUCF	2.9
HC-PC	3.0

S20 Comparison of the spectra of C1s, O1s, N1s, Si2p and I3d of the HC-FSD and HC-FSD-5Cy samples

Figure S20. Comparison of the spectra of C 1s, O1s, N1s, Si 2p and I 3d of the HC-FSD and HC-FSD-5Cy samples



Bibliography

- 1 J. L. Vidal, V. P. Andrea, S. L. MacQuarrie and F. M. Kerton, *ChemCatChem*, 2019, **11**, 4089–4095.
- 2 V. B. Saptal, T. Sasaki, K. Harada, D. Nishio-Hamane and B. M. Bhanage, *ChemSusChem*, 2016, **9**, 644–650.
- 3 D. H. Lan, L. Chen, C. T. Au and S. F. Yin, *Carbon N. Y.*, 2015, **93**, 22–31.
- 4 K. R. Roshan, T. Jose, A. C. Kathalikkattil, D. W. Kim, B. Kim and D. W. Park, *Appl. Catal. A Gen.*, 2013, **467**, 17–25.
- 5 X. Wu, M. Wang, Y. Xie, C. Chen, K. Li, M. Yuan, X. Zhao and Z. Hou, *Appl. Catal. A Gen.*, 2016, **519**, 146–154.
- 6 Z. Wu, H. Xie, X. Yu and E. Liu, *ChemCatChem*, 2013, **5**, 1328–1333.
- 7 X. Xiong, H. Zhang, S. L. Lai, J. Gao and L. Gao, *React. Funct. Polym.*, 2020, **149**, 104502.
- 8 S. Lai, J. Gao, H. Zhang, L. Cheng and X. Xiong, *J. CO₂ Util.*, 2020, **38**, 148–157.
- 9 J. Tharun, Y. Hwang, R. Roshan, S. Ahn, A. C. Kathalikkattil and D. W. Park, *Catal. Sci. Technol.*, 2012, **2**, 1674–1680.
- 10 M. Borjian Boroujeni, M. S. Laeini, M. T. Nazeri and A. Shaabani, *Catal. Letters*, 2019, **149**, 2089–2097.
- 11 S. Kumar, K. Prasad, J. M. Gil, A. J. F. N. Sobral and J. Koh, *Carbohydr. Polym.*, 2018, **198**, 401–406.
- 12 C. Guizani, M. Jeguirim, S. Valin, L. Limousy and S. Salvador, *Energies*, 2017, **10**, 796.
- 13 R. Sun, X. Zhang, C. Wang and Y. Cao, *J. Environ. Chem. Eng.*, 2021, **9**, 105368.
- 14 C. Nieto-Delgado, F. S. Cannon, Z. Zhao and P. G. Nieto-Delgado, *Fuel*, 2021, **298**, 120816.
- 15 R. M. Silverstein, F. X. Webster and D. J. Kiemle, *John Wiley Sons, Inc*, 2005.
- 16 L. T. Cuba-Chiem, L. Huynh, J. Ralston and D. A. Beattie, *Langmuir*, 2008, **24**, 8036–8044.
- 17 A. O. Odeh, *Ranliao Huaxue Xuebao/Journal Fuel Chem. Technol.*, 2015, **43**, 129–137.
- 18 C. Samorí, C. Torri, D. Fabbri, G. Falini, C. Faraloni, P. Galletti, S. Spera, E. Tagliavini and G. Torzillo, *ChemSusChem*, 2012, **5**, 1501–1512.
- 19 S. Pradhan, J. Hedberg, J. Rosenqvist, C. M. Jonsson, S. Wold, E. Blomberg and I. O. Wallinder, *PLoS One*, 2018, **13**, 1–24.
- 20 C. J. Pouchert, *The Aldrich library of FT-IR spectra.*, Aldrich, Milwaukee, Wis, Ed. 2., 1975.
- 21 C. Le Losq, G. D. Cody and B. O. Mysen, *Am. Mineral.*, 2015, **100**, 945–950.